# Photopolymerization of Ternary Thiol–Ene/Acrylate Systems: Film and Network Properties

HUANYU WEI,[1] ASKIM F. SENYURT,[1] SONNY JÖNSSON,[2] CHARLES E. HOYLE[1]

[1]School of Polymers and High Performance Materials, University of Southern Mississippi, 118 College Drive, 10076, Hattiesburg, Mississippi 39406

[2]Fusion UV Systems, Incorporated, Gaithersburg, Maryland 20878

*Received 5 September 2006; accepted 23 October 2006*
*DOI: 10.1002/pola.21844*
*Published online in Wiley InterScience (www.interscience.wiley.com).*

**ABSTRACT:** Photocurable, ternary-component mixtures of a 1:1 molar multifunctional thiol–ene (trithiol and triallyl ether) blend and a 16-functional acrylate based monomer have been photopolymerized, and the final film properties of the ternary crosslinked networks have been measured. The photopolymerization kinetics, morphology, and mechanical and physical properties of the films have been investigated with real-time infrared, atomic force microscopy, and dynamic mechanical analysis. The photopolymerization process is a combination of acrylate homopolymerization and copolymerizations of thiol with allyl ether and acrylate functionalities. The tan $\delta$ peaks of the photopolymerized ternary systems are relatively narrow and tunable over a large temperature range. The morphology is characterized by a distinct phase-separated nanostructure. The photocured thiol–ene/acrylate ternary systems can be made to exhibit good mechanical properties with enhanced energy absorption at room temperature by the appropriate selection of each component concentration. © 2007 Wiley Periodicals, Inc. J Polym Sci Part A: Polym Chem 45: 822–829, 2007

**Keywords:** films; kinetics (polym.); photopolymerization; ternary thiol–ene/acrylate

## INTRODUCTION

The photopolymerization of thiol–ene and acrylate monomers to produce crosslinked networks has been the focus of many studies. In traditional thiol–ene systems, the enes react only with the thiol and cannot participate in a homopolymerization process. Thiol–ene systems polymerize by a free-radical step-growth process that forms highly uniform crosslinked networks with very narrow glass transitions.[1] Shrinkage occurs to a great extent in the liquid state because of the high monomer conversion at the gel point corresponding to thiol–ene network formation.[1] By contrast, early gelation in acrylate polymerization forms inhomogeneous high-density regions.[2–5] It has been assumed that these high-density, ball-like structures coalesce and form more organized structures at high conversions.[2,4–6] Cramer and Bowman[7] showed that mixtures of multifunctional thiols and multifunctional acrylates alter the inherent acrylate chain growth polymerization process and have a profound effect on the mechanical properties of the cured films because of the formation of more uniform networks. Essentially, the acrylate participates in a copolymerization process with the thiol, thereby acting as an ene. In addition, the acrylate homopolymerizes. Because there are a

*Correspondence to:* C. E. Hoyle (E-mail: charles.hoyle@usm.edu)

Journal of Polymer Science: Part A: Polymer Chemistry, Vol. 45, 822–829 (2007)

large number of acrylate monomers available, thiol–acrylate combinations can be made to achieve a variety of properties, depending on the structures and concentrations of each.

Considering this description of traditional thiol–ene and thiol–acrylate systems and the corresponding potential for achieving a variety of physical and mechanical properties, one can argue that mixtures of multifunctional thiols with both traditional enes that do not homopolymerize and acrylates that copolymerize with the thiol and homopolymerize present an even greater opportunity for fabricating networks with a tailored set of properties. The photoinitiated polymerization kinetics of ternary thiol–ene/acrylate systems has indeed been reported previously.[8] Recently, it has been found that the photopolymerization of acrylate and thiol–ene mixtures form networks with mechanical properties that are tunable by the concentration of the acrylate used.[9] The peak maximum in plots of tan $\delta$ versus the temperature has been shown to vary over a wide range, depending on the concentration of acrylate in the prepolymerization mixture. The magnitude of the tan $\delta$ peak maximum in photopolymerized ternary systems is close to that obtainable by traditional thiol–ene or ternary thiol–ene–ene systems. However, because of limitations in the availability of traditional enes that are both reactive and rigid, the temperature range over which the peak maximum of thiol–ene and thiol–ene–ene systems can be tuned is limited compared with that for ternary thiol–ene/acrylates. Also, for thiol–ene/acrylate ternary systems, because the structures and concentrations of each component can be varied, the potential for selectively altering other physical, mechanical, and optical properties while achieving a high tan $\delta$ value is excellent. The formulation latitude in creating films and thermoset plastics with a specific set of physical, mechanical, and optical properties is therefore maximized by ternary systems.

In view of the previous discussion and to provide an illustration of ternary thiol–ene/acrylate photopolymerization, we present results herein for a single representative ternary thiol–ene/acrylate system. Our preliminary communication, which introduced the ternary concept with respect to mechanical and morphological implications, focused primarily on the basic dynamic mechanical analysis (DMA) and energy impact absorption of 4-mm-thick plates (not films).[9] Here we report an expanded analysis of the thermal and physical properties of relatively thin films made from a selected ternary thiol–ene acrylate system as well as impact results for thick plates. This work combines DMA, differential scanning calorimetry (DSC), and atomic force microscopy (AFM) with traditional film physical property measurements such as hardness, adhesion, fracture crack propagation, and front and reverse impact to provide a complete description of the film properties. A general kinetic description of the reactive group conversions as a function of time is also given. Previously, we used a tertiary acrylate that, upon photopolymerization with a thiol–ene, gave networks with tan $\delta$ peak maxima that were $\sim$60 °C or less.[9] Here we have selected a 16-functional acrylate (based on a hyperbranched polyester structure) that itself has an inherent peak maximum in a plot of tan $\delta$ versus the temperature of almost 120 °C. This allows for the production of films and plates from ternary thiol–ene/acrylate mixtures that have substantially higher glass transitions than reported previously.[9] Hyperbranched molecules with acrylate, vinyl ether, allyl ether, or epoxy end groups have been studied as multifunctional crosslinking systems for use in UV coatings,[10–12] and thus there is ample precedence for their use as components in film-forming systems.

## EXPERIMENTAL

Allyl pentaerythritol (APE), trimethylolpropane tris(3-mercaptopropionate) (TriThiol), and an acrylate with an average functionality of 16 (designated 16Acrylate) were kindly supplied by Perstorp Specialty Chemicals, Bruno Bock Co., and Sartomer Co., respectively. 2,2-Dimethoxy-2-phenyl acetophenone (DMPA) was obtained from Ciba Specialty Chemicals. All reagents were used without further purification.

Thiol–ene mixtures were prepared by the blending of TriThiol with APE on the basis of equal molar functional groups. 16Acrylate was added to the TriThiol–APE system (0, 20, 40, 50, 60, 80, or 100 mol %) to prepare seven different TriThiol–APE/16Acrylate mixtures. The amount of the UV initiator, DMPA, in each case, was 1 wt %. Films on glass plates (200 $\mu$m) and steel Q panels (125 $\mu$m) were cured on a Fusion curing line system with a D bulb (3.0 W/cm$^2$, belt speed = 3.05 m/min, five passes). Thick samples (4-mm thick) were irradiated with a low-intensity, 254-nm, low-pressure mercury

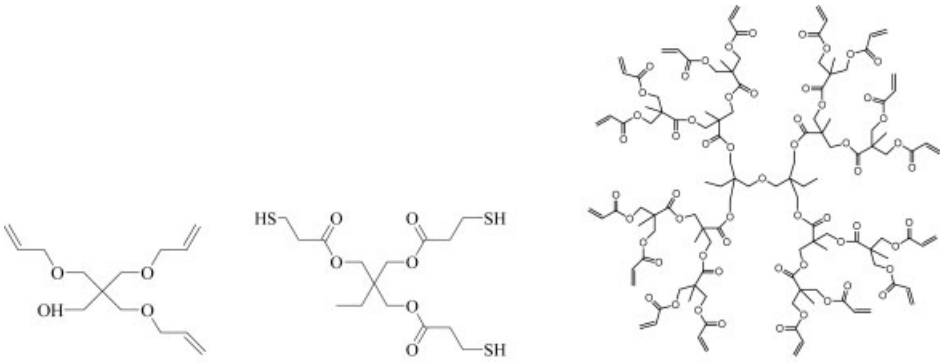


a b c

**Figure 1.** Chemical structures of (a) APE, (b) TriThiol, and (c) 16Acrylate.

lamp (0.1 mW/cm$^2$) in air; we stress that the samples were processed to prevent a high-temperature rise during polymerization by the exposure of the samples for short intervals to the low-intensity lamp during the initial polymerization stage. Special precautions were taken to reduce oxygen inhibition in the polymerization of pure 16Acrylate.

The thermal transitions of the films were recorded with both a TA Q800 dynamic mechanical analyzer and a TA Q1000 differential scanning calorimeter. DMA was conducted in the shear sandwich mode for 10 $\times$ 10 mm$^2$ samples with thicknesses of 150–200 $\mu$. We have chosen to quote the tan delta maximum as the glass transition temperature, $T_g$ Freestanding film samples, obtained by the removal of cured films from glass substrates, were heated from $-100$ to 300 °C at a rate of 3 °C/min and at a frequency of 1 Hz. For DSC measurements, the samples were heated from $-50$ to 100 °C at a rate of 10 °C/min.

The photopolymerization kinetic profiles during the UV-induced free-radical polymerizations were obtained with real-time infrared (RTIR). Infrared spectra were recorded on a modified Bruker 88 Fourier transform infrared spectrometer designed to allow light to impinge on a horizontal sample with a fiber-optic cable as a function of the irradiation time. A 200-W, high-pressure mercury–xenon lamp (Oriel Co.) served as the light source to induce the free-radical polymerization. The conversion rates of each carbon–carbon double bond were monitored at 812 cm$^{-1}$ for acrylate, at 3080 cm$^{-1}$ for allyl ether, and at 2570 cm$^{-1}$ for thiol bands.

A surface topography analysis of cross sections of the freeze-fractured samples was conducted with an atomic force microscope (MultiMode atomic force microscope from Veeco Instruments, Inc., Santa Barbara, CA; Tapping mode etched silicon probes with a nominal resonance frequency of 275 kHz in the tapping mode).

A Tinius Olsen instrument (model 92T) modified to measure the energy absorbed upon a moderate impact (energy = 1.13 J) with a steel head was used to investigate the impact resistance of 4-mm-thick samples. A thick metal plate was placed behind two 4-mm plates, and the energy lost upon impact was estimated by the maximum return angle of the pendulum after the impact. The absorbance values may have differed from those obtained with other sample thicknesses and impact configurations. For the films, the Persoz pendulum hardness was measured with a BYK Gardner pendulum hardness tester. Crosscut tape test adhesion measurements of the films cast on steel Q panels were conducted according to ASTM D 3359-02. Mandrel bend testing (cracking and elongation) for steel Q panel cast films was conducted according to ASTM D 522, and rapid deformation (impact) was measured according to ASTM D 2794-93.

## RESULTS AND DISCUSSION

This article focuses on the photopolymerization of ternary systems involving the three components in Figure 1: a trithiol (designated TriThiol), a triallyl ether (designated APE), and a 16-functional acrylate (designated 16Acrylate). Mixtures were prepared by the blending of

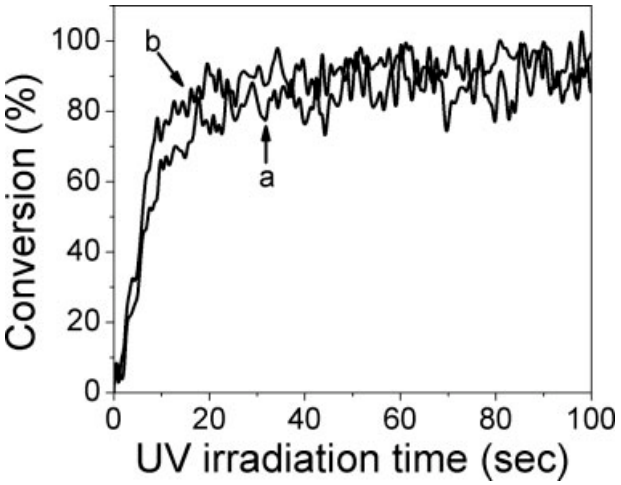


**Figure 2.** RTIR plots of the conversion percentage versus time for TriThiol–APE: (a) thiol and (b) allyl ether. The light intensity (full arc) was 1.87 mW/cm$^2$.

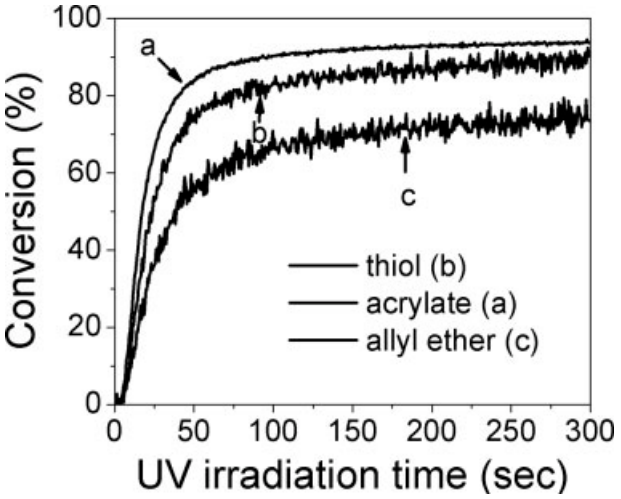


**Figure 4.** RTIR plots of the conversion percentage versus time for TriThiol–APE with 50 mol % 16Acrylate: (a) acrylate, (b) thiol, and (c) allyl ether. The light intensity (full arc) was 1.87 mW/cm$^2$.

TriThiol with APE on the basis of equal molar functional groups and the subsequent addition of increasing molar concentrations of 16Acrylate. Each mixture contained 1 wt % DMPA, the cleavage photoinitiator.

Kinetic analyses were conducted with RTIR. The resultant plots of the conversion versus the UV irradiation time for TriThiol–APE, 16Acrylate, and TriThiol–APE with 50 mol % 16Acrylate are shown in Figures 2–4, respectively. For the TriThiol–APE system, without any added 16Acrylate, the thiol and allyl ether essentially copolymerized, reaching about 95% conversion with no induction period. On the other hand, for pure 16Acrylate, there was about a 12-s oxygen inhibition period not seen for the TriThiol–APE system. Also, the pure 16Acrylate polymerized more slowly than TriThiol–APE and reached a conversion of only about 75%. Johansson and Hult[10] showed that the polymerization of a similar multifunctional, hyperbranched acrylate resulted in multiple acrylate groups reacting internally on the same molecule. When 50 mol % 16Acrylate was combined with a 1:1 molar mixture of TriThiol and APE, oxygen inhibition was greatly reduced. Moreover, the acrylate photopolymerized faster than the thiol and allyl ether groups and obtained greater than 94% conversion, which was much higher than the 75% conversion attained for 16Acrylate alone. The thiol (TriThiol) and allyl ether (APE) attained 90 and 73% conversions, respectively. Considering a 1:1 thiol and allyl ether copolymerization, we conclude that copolymerization between the thiol groups on TriThiol and the acrylate groups on 16Acrylate occurs. Overall, the photopolymerization of TriThiol–APE with 50 mol % 16Acrylate proceeds by a combination of acrylate homopolymerization and thiol–ene copolymerizations between thiol–allyl ether and thiol–acrylate groups.

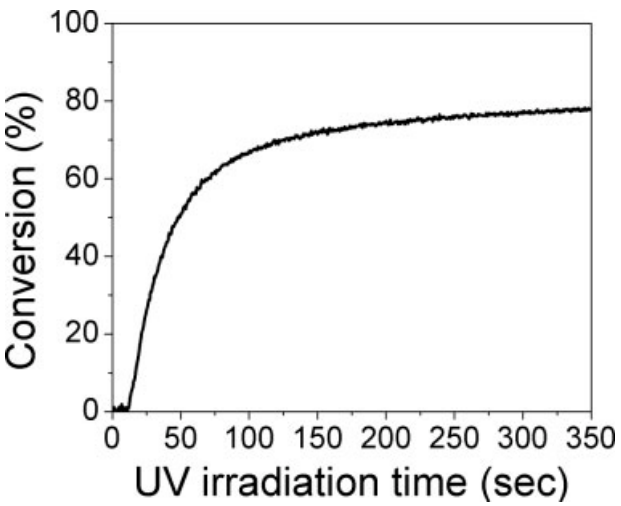


**Figure 3.** RTIR plots of the acrylate conversion percentage versus time for 16Acrylate. The light intensity (full arc) was 1.87 mW/cm$^2$.

The thermal and mechanical properties of the photopolymerized films of TriThiol–APE, 16Acrylate, and ternary TriThiol–APE/16Acrylate

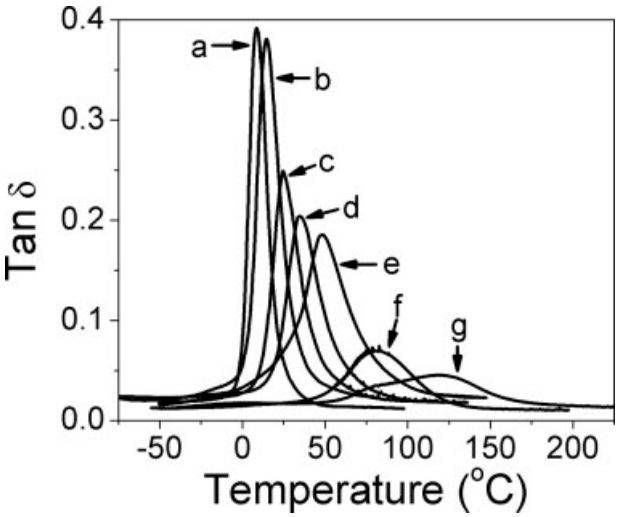


**Figure 5.** Plots of tan $\delta$ versus temperature for films formed from (a) pure TriThiol–APE, (b–f) mixtures of TriThiol–APE with 16Acrylate with (b) 20, (c) 40, (d) 50, (e) 60, and (f) 80 mol % concentrations, and (g) pure 16Acrylate.

mixtures with different molar percentage ratios of 16Acrylate (20, 40, 50, 60, and 80%) were characterized with DMA and DSC (shown in Figs. 5 and 6, respectively). The DMA first-scan results clearly show that, on the one hand, the TriThiol–APE films has a glass transition region with a very narrow tan $\delta$ peak representing a uniform network matrix resulting from a free-radical step-growth process. On the other hand, the film produced from 16Acrylate had a broad tan $\delta$ plot indicative of a very heterogeneous network matrix with a main peak maximum around 118 °C and a very small peak around 0 °C. All the films formed by the polymerization of samples with 20, 40, 50, 60, or 80 mol % 16Acrylate yielded relatively symmetrical plots of tan $\delta$ versus the temperature in comparison with the sample formed by the photopolymerization of pure 16Acrylate. However, the width of tan $\delta$ broadened and the height decreased continuously with increasing 16Acrylate concentration. Hence, it can be readily concluded that, on a mechanical/thermal basis, the matrix uniformity increases with the TriThiol–APE content. There was no indication of any shoulders in the plot of tan $\delta$ versus the temperature for the film made from only TriThiol–APE. To characterize the thermal transitions, DSC scans, shown in Figure 6, were also recorded for each sample. The film from Trithiol–APE had a very narrow glass-transition region, whereas $T_g$ of the glass transition region photopolymerized 16Acrylate was barely detectable. With the addition of 20, 40, 50, 60, and 80 mol % 16Acrylate, the glass-transition region progressively broadened. The DSC results essentially paralleled the DMA results. The $T_g$ values from DMA and DSC measurements plotted versus the molar concentration of 16Acrylate in Figure 7 clearly show that $T_g$, as measured by DMA and DSC, increases continuously with an increasing 16Acrylate concentration.

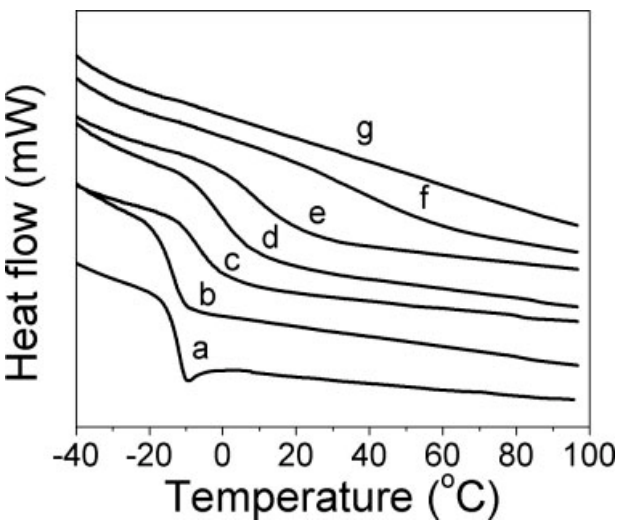


**Figure 6.** DSC plots for films formed from (a) pure TriThiol–APE, (b–f) mixtures of TriThiol–APE with 16Acrylate with (b) 20, (c) 40, (d) 50, (e) 60, and (f) 80 mol % concentrations, and (g) pure 16Acrylate.

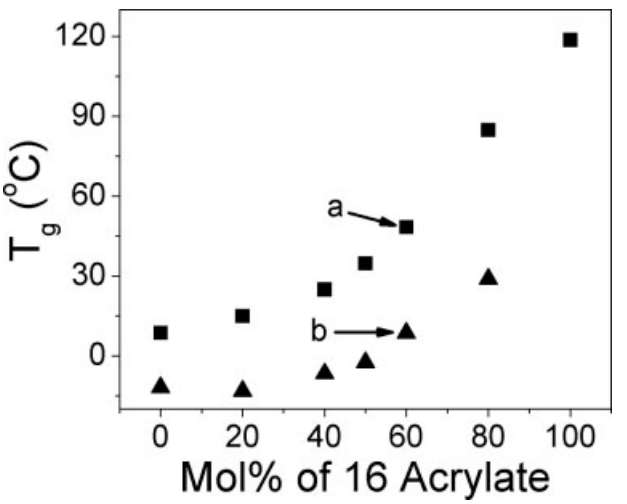


**Figure 7.** $T_g$ measured by both (a) DMA and (b) DSC for TriThiol–APE/16Acrylate ternary systems as a function of the 16Acrylate molar percentage.

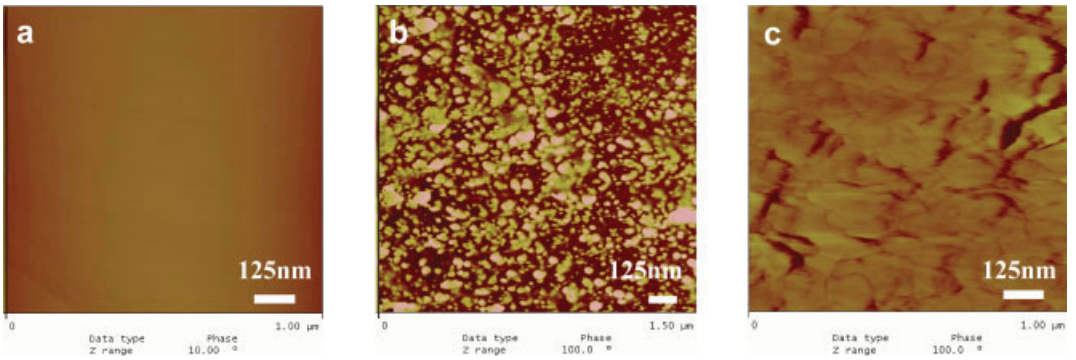


**Figure 8.** Phase images of cross sections of (a) TriThiol–APE, (b) TriThiol–APE with 50 mol % 16Acrylate, and (c) a 16Acrylate film. [Color figure can be viewed in the online issue, which is available at www.interscience.wiley.com.]

It is clear from the results in Figure 5 that the films prepared by the photopolymerization of the ternary mixtures of a 1:1 molar TriThiol–APE system with 16Acrylate did not experience phase separation on a scale that would result in greatly altered macroscopic mechanical properties. Nonetheless, we think it important that a complete description of the film morphology on the nanoscopic scale be presented. Therefore, morphological studies of films of Trithiol–APE, TriThiol–APE with 50 mol % 16Acrylate, and 16Acrylate were conducted by AFM in the tapping mode. The AFM analysis (Fig. 8) of a cross section of freeze-fractured, 4-mm-thick plates containing 50 mol % 16Acrylate (with no surface treatment) clearly shows at room temperature a phase-separated morphology indicated by light and dark phase-separated regions on the scale of 10–130 nm. It is reasonable to speculate that the phases indicated by the lighter regions (i.e., harder regions) are rich in reacted acrylate groups. The nanostructure in Figure 8 is similar to that reported recently[9] for a ternary system composed of TriThiol–APE and a triacrylate. The AFM analysis of 4-mm-thick plates formed by the photopolymerization of pure TriThiol–APE and pure 16Acrylate shows little variation in the hardness (modulus) and thus no indication of the phase-separated morphology found for the ternary mixture. At this time, we do not know the physical and mechanical consequences of the nanophase structure. However, the ramifications of the nanophase structure are currently being investigated with a variety of techniques, including gas transport and moisture uptake. We simply point out its existence.

The Persoz hardness of the UV-cured films of TriThiol–APE, 16Acrylate, and TriThiol–APE/16Acrylate mixtures were also evaluated (Fig. 9). Both the TriThiol–APE and 16Acrylate-based films had much higher Persoz hardness values than their mixtures, with minimum damping times recorded for the mixtures containing 50 or 60 mol % 16Acrylate: the minimum in the Persoz hardness corresponds to a maximum in the energy damping. The low Persoz values indicate the maximization of energy damping for samples having 40–60 mol % 16Acrylate, which correspond to samples that have large tan $\delta$ values at room temperature. To verify the Persoz results, the energy absorbance upon impact by a

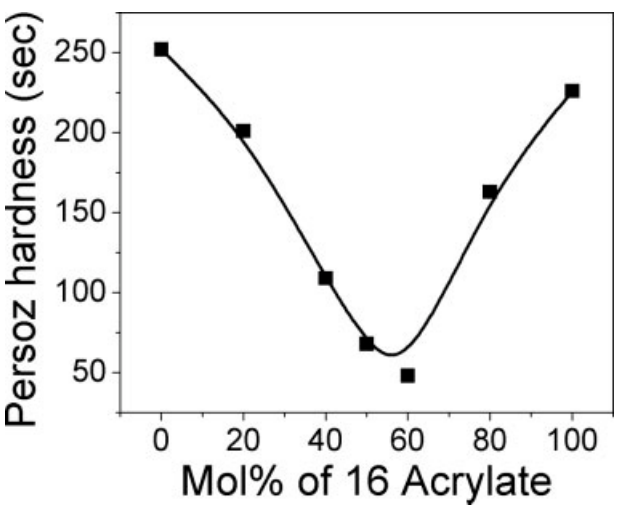


**Figure 9.** Persoz hardness plot of TriThiol–APE/16Acrylate ternary systems as a function of the 16Acrylate molar percentage.

**Table 1.** Mechanical Properties of the Films Fabricated from TriThiol–APE, 16Acrylate, and TriThiol–APE with 50 mol % 16Acrylate

| | TriThiol–APE | Trithiol–APE with 50 mol % 16Acrylate | 16Acrylate |
|---|---|---|---|
| Energy absorbance (plate) | 0.41 J (36%) | 0.77 J (68%) | 0 J (shattered) |
| Pencil hardness (film) | B | 4H | 8H |
| Adhesion (film) | 0B (17.25% remained) | 0B (12.7% remained) | 0B (0% remained) |
| Cracking (film) | 4.95 cm | 5.87 cm | 13.82 cm |
| Elongation (film) | 7.55% | 6.50% | 3.70% |
| Front impact (film) | 4.75 J | 6.78 J | 3.16 J |
| Reverse impact (film) | 1.13 J | 0.68 J | 0.45 J |

metal head was measured with a Tinius Olsen impact test (Table 1) for 4-mm-thick plates of TriThiol–APE, TriThiol–APE with 50 mol % 16Acrylate, and 16Acrylate fabricated by photopolymerization with a low-intensity, low-pressure mercury lamp (see the Experimental section). Although the plate from the TriThiol–APE mixture absorbed ~36% of the impact energy of a striking head, the plate from pure 16Acrylate was brittle and shattered upon impact. However, TriThiol–APE with 50 mol % 16Acrylate exhibited an energy absorbance of ~68%. The energy absorption depends on the value of tan $\delta$ (at the frequency of the energy impact) at a given temperature. It is thus not surprising that the plate composed of TriThiol–APE with 50 mol % 16Acrylate had a relatively high energy absorption at room temperature, at which it had high tan $\delta$ values (see the 1-Hz DMA analysis in Fig. 5). We point out that, as indicated in the introduction, it is certainly possible to make a network from a thiol–ene or thiol–ene–ene system that has a high tan $\delta$ peak maximum at the impact measurement temperature and high energy absorption. However, we reiterate here that ternary systems offer the ability to tune the tan $\delta$ peak maximum over a large temperature range. Furthermore, the nature of the acrylate can be varied to adjust and maximize other network chemical and physical properties while high impact absorption is maintained at a given temperature. Finally, as a note of interest, the amount of energy absorbed by the ternary system described herein is much greater than that for traditional materials used in sporting applications; that is, commercial ethylene vinyl acetate based materials typically absorb approximately 40–50% of a 1.13-J impact near room temperature under the same conditions employed here. It is possible to obtain even higher energy-absorbance values by the variation of the components in the ternary system. This will be the subject of a future report.

In accordance with the premise for the investigation of ternary thiol–ene/acrylate set forth in the introduction, other properties such as the pencil hardness, adhesion, flexibility (cracking resistance and elongation), and front and reverse impact were also investigated for films made from TriThiol–APE, TriThiol–APE with 50 mol % 16Acrylate, and 16Acrylate. As can be seen in Table 1, the pencil harness increases with increasing 16Acrylate content, whereas the adhesion decreases. This is consistent with an increase in the glass transition temperature and room-temperature modulus with the acrylate concentration. The cracking resistance/elongation data illustrate a concomitant decrease in the flexibility with the acrylate concentration, and this is consistent with the decrease found for the values of the reverse impact. The films obtained from pure TriThiol–APE also had somewhat better adhesion to a steel plate, although we note that none of the evaluated films exhibited what would be classified as good adhesion to steel. Finally, we note that the front impact was highest for the film based on the ternary TriThiol–APE with 50 mol % 16Acrylate system, and this was consistent with the low value for the Persoz hardness damping (Fig. 9) and the high energy absorption found for the 4-mm plates made from the ternary mixture. If other multifunctional acrylates were used instead of 16Acrylate, material networks with the same energy-absorbing properties could be obtained, but variations in other physical properties such as the hardness, adhesion, flexibility, and fracture toughness would occur.

## CONCLUSIONS

An analysis of photopolymerized ternary thiol–allyl ether/acrylate mixtures has resulted in narrow mechanical/thermal transition regions. The temperature corresponding to the peak maximum in tan $\delta$ varies with the acrylate concentration and can be adjusted to have a maximum at any temperature within the boundaries of the $T_g$ values of the pure materials. This provides flexibility for making materials with high energy-absorbing properties tuned for maximum performance at a given temperature. The ternary systems are characterized by a phase-separated nanoscopic morphology. There is no evidence at this time that the phase-separated morphology is crucial in shaping the film macroscopic mechanical and physical properties; however, this subject is still under investigation. Future reports will focus on the effect of the acrylate structure on altering physical and mechanical properties while high impact energy absorption is maintained.

The authors thank the Materials Research Science and Engineering Center (MRSEC) program of the National Science Foundation (award no. DMR 0213883) and Fusion UV Systems for their support. Perstorp, Bruno Bock, Sartomer, and Ciba Specialty Chemicals are also acknowledged for providing samples.

## REFERENCES AND NOTES

1. Hoyle, C. E.; Lee, T. Y.; Roper, T. J Polym Sci Part A: Polym Chem 2004, 42, 5301.
2. Kloosterboer, J. G. Adv Polym Sci 1988, 84, 8.
3. Kloosterboer, J. G.; Van de Hei, G. M.; Boots, H. M. J Polym Commun 1984, 25, 354.
4. Bowman, C. N.; Anseth, K. S. Macromol Symp 1995, 93, 269.
5. Dusek, K. In Developments in Polymerization 3; Harvard, R. N., Ed.; Applied Science: London, 1982; Vol. 3, Chapter 4.
6. Dusek, K.; Galina, H.; Mikes, J. Polym Bull 1980, 3, 19.
7. Cramer, N. B.; Bowman, C. N. Polym Prepr (Am Chem Soc Div Polym Chem) 2003, 44, 17.
8. Reddy, S. K.; Cramer, N. B.; Bowman, C. N. Macromolecules 2006, 39, 3681.
9. Senyurt, A. F.; Wei, H.; Phillips, B.; Cole, M.; Nazarenko, S.; Hoyle, C. E.; Piland, S. G.; Gould, T. E. Macromolecules 2006, 39, 6315–6317.
10. Johansson, M.; Hult, A. J Coat Technol 1995, 67, 35.
11. Shi, W. F.; Rånby, B. J Appl Polym Sci 1996, 59, 1937.
12. Sangermano, M.; Malucelli, G.; Bongiovanni, R.; Priola, A.; Harden, A.; Rehnberg, N. Polym Eng Sci 2003, 43, 1460.